Computational Fluid Dynamics Ventilation Study for the Human Powered Centrifuge at the International Space Station

Chang H. Son[1]
The Boeing Company, Houston, TX, 77059, United States

The Human Powered Centrifuge (HPC) is a facility that is planned to be installed on board the International Space Station (ISS) to enable crew exercises under the artificial gravity conditions. The HPC equipment includes a "bicycle" for long-term exercises of a crewmember that provides power for rotation of HPC at a speed of 30 rpm. The crewmember exercising vigorously on the centrifuge generates the amount of carbon dioxide of about two times higher than a crewmember in ordinary conditions. The goal of the study is to analyze the airflow and carbon dioxide distribution within Pressurized Multipurpose Module (PMM) cabin when HPC is operating. A full unsteady formulation is used for airflow and CO_2 transport CFD-based modeling with the so-called sliding mesh concept when the HPC equipment with the adjacent Bay 4 cabin volume is considered in the rotating reference frame while the rest of the cabin volume is considered in the stationary reference frame. The rotating part of the computational domain includes also a human body model. Localized effects of carbon dioxide dispersion are examined. Strong influence of the rotating HPC equipment on the CO_2 distribution detected is discussed.

I. Introduction

FOR the long-duration space missions effects of weightlessness on the human body are essential. The consequences of long-term weightlessness include undesirable physiological adaptations that influence the ability of astronauts to function efficiently upon the return to an environment with gravity.[1] Artificial gravity has the potential to fully mitigate the physiological deconditioning that results from long-term exposure to weightlessness.[2] Potential benefits of artificial gravity generated by a human powered centrifuge (HPC). have been investigated recently, and several HPC concepts have been described in the literature.[2,3] In HPC the effects of artificial gravity and exercise are combined while an astronaut exercises, usually by pedaling, on a centrifuge device. These systems require no external power, being operated by the subjects themselves. Combination of exercises and simulated gravity simultaneously prevents muscle atrophy, bone demineralization, and cardiovascular detraining. The hemodynamic and metabolic responses to increased loading provided by a human-powered centrifuge have been described in detail in Ref. 4.

The HPC that is planned to be installed on board the International Space Station (ISS) includes a "bicycle" for long-term exercises of a crewmember that provides power for rotation of HPC at a speed of 30 rpm. The crewmember exercising vigorously on the centrifuge generates the amount of carbon dioxide much higher than a crewmember in ordinary conditions. Maintaining cabin air quality is a key issue for crew comfort and safety, and it is necessary to make sure that the ISS ventilation systems are enough to supply clean air to the crew exercising with the HPC.

It is suggested to install the HPC in the Pressurized Multipurpose Module (PMM).[5] The goal of the study is to find out the evolution of the CO_2 distribution in the PMM cabin atmosphere in case of crew is exercising under the artificial gravity conditions. Numerical modeling have been performed with the Computational Fluid Dynamics (CFD) technique using the ANSYS FLUENT 12.1.4 CFD software.[6]

II. Computational Model

A. Cabin Aisle Way Geometry Model and Airflow Boundary Conditions

The 3D geometry model of the PMM aisle way adopted for the present CFD analysis of the cabin ventilation is also illustrated in Fig. 1. Views from aft to forward direction are shown in Fig. 1b, while a view from nadir to zenith direction is shown in Fig. 1c. Fig. 1d also gives an illustration of four slices used for field post-processing. When HPC is in operation, the CTB are assumed to be stacked in one layer only in the front of each rack for Bay 1, 2, and 3. Bay 4 is free from stowage, and all the panels are removed for Bay 4 as well. The HPC equipment installed in Bay 4 is marked by green in Fig. 1b, 1c, and 1d. The total volume of the PMM cabin aisle way considered is 34 m^3.

Two crew-member models, ECLOIDs (Environmental Control and Life Support System – ECLSS – AndrOID), are incorporated into the PMM geometry model. The first ECLOID simulates an exercising crew placed at HPC bike. The second ECLOID simulates an assisting crew that monitors and records all the activities of the centrifuge and could help the exercising person in case of emergency. The assisting ECLOID is placed in Bay 2 faced to the nadir direction (to endcone).

When the crewmember in Bay 4 is exercising, the HPC bike is rotating rapidly together with the human body. The constant angular speed of 30 rpm is kept that corresponds to one revolution per two seconds. The direction of rotation with respect to the human body position is indicated in Fig. 1b.

The active inlet/outlet boundaries are also shown in Fig. 1 (the inlets for the cabin are marked by blue color, while the outlets are colored by red). The PMM ventilation system includes eight air supply diffusers, two endcone diffusers (the flow restrictors), and eight return grilles.

Eight air supply diffusers are placed in standoffs stretched under the ceiling in the longitudinal direction (in the nadir-zenith direction). Each PMM cabin air supply diffuser has a given flow rate of 26.88 cfm that corresponds to the total supply flow rate of 215 cfm. Additionally, PMM ventilation system is supplied with two endcone diffusers that are visible at the end of the duct bends in Fig. 1. The endcone diffusers direct the airflow in the aft-forward direction and form a circulation loop in the endcone region. Each PMM endcone air supply diffuser has a given flow rate of 15 cfm that corresponds to the total supply flow rate of 30 cfm.

Eight PMM return grilles are placed at the deck. The flow rate leaving the PMM cabin through each return grille is 14.375 cfm, so that the total flow rate is 115 cfm. The hatch from PMM to Node 1 is open. The IMV flow rate leaving the PMM interior through the hatch is 130 cfm. The clean IMV air returns back to PMM from Node 1 through the ducting system. It is mixed with the air from the return grilles, and the total 245 cfm of air are supplied to the inlet diffusers.

The inlet/outlet velocity boundary conditions are set with the uniform inlet velocity approximation adopted for each inlet diffuser. The velocity magnitude for each diffuser is defined by a corresponding volumetric flow rate and an effective area of the diffuser. The inlet airflow is supposed to be normal to the boundary. As well, the uniform velocity boundary condition is imposed for each return grille and the PMM/Node 1 hatch surface. A no-slip boundary condition is imposed on all of the solid ISS surfaces.

The air density is computed using the ideal gas law for an incompressible flow. In this form, the density depends only on the operating pressure and not on the local relative pressure field.

Airflow was computed for two different cases. Case 1 was computed for the static HPC without rotation. Case 2 was computed for the rotating HPC using the unsteady sliding mesh model.[6] The sliding model concept implies that the computational domain is divided into two parts. The first part is a cylinder in Bay 4 containing the rotating HPC equipment and the exercising ECLOID with the adjacent. It is considered in the rotating reference frame. The remaining part of the cabin volume is considered in the stationary reference frame. At each time step the flux across the sliding interface between these two parts is computed.

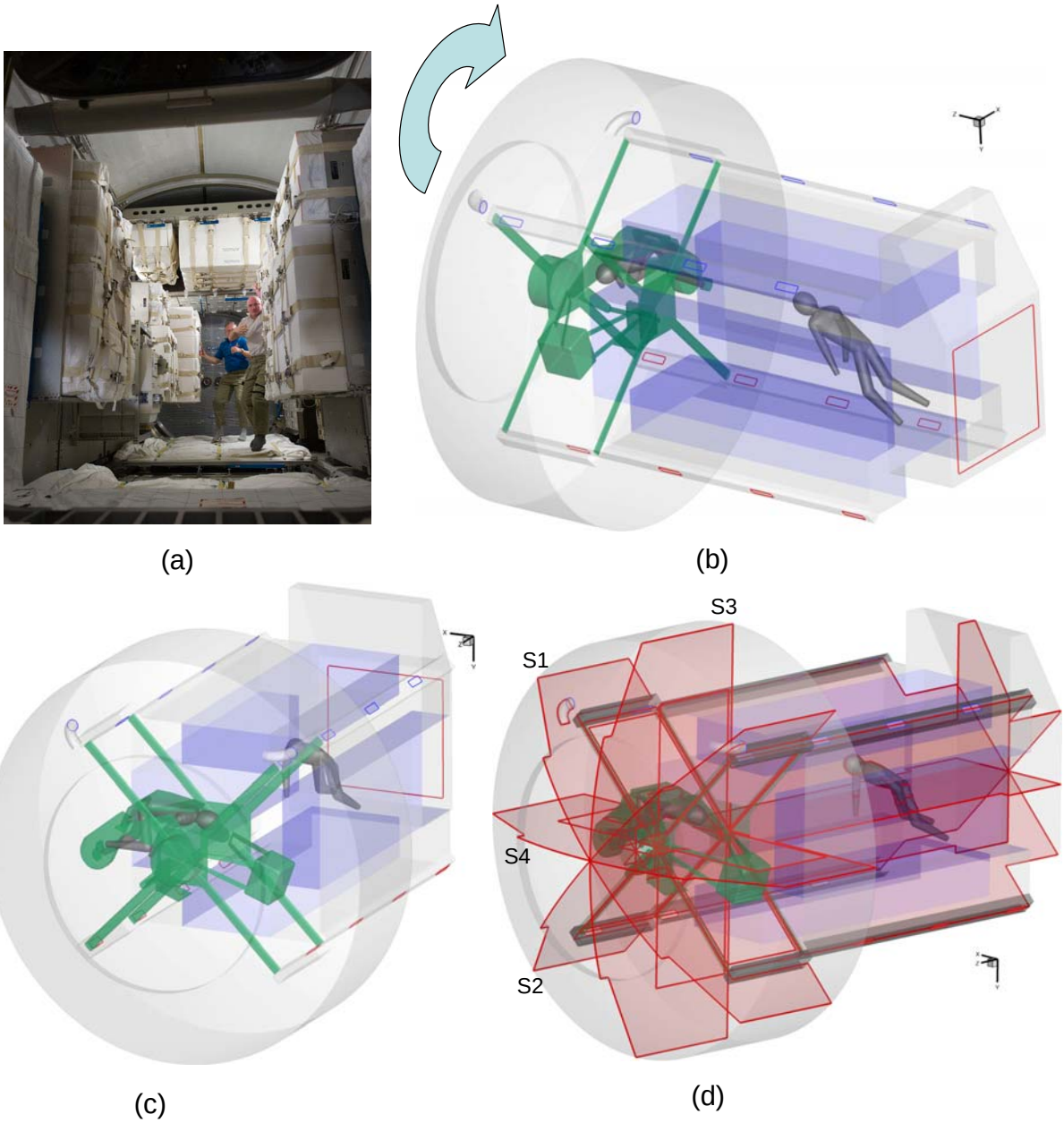

Figure 1. (a) Interior of PMM after its installation in ISS[7]; (b-d) views of the geometry model used for CFD study of CO_2 transport in PMM when crew is exercising on HPC.

B. Carbon Dioxide Transport Problem Formulation

The transient CO_2 transport problem with prescribed uniform initial partial pressure of carbon dioxide ($ppCO_2$) was computed with the "frozen" velocity field approach, i.e. the scalar field is transported by the steady-state or an instantaneous airflow field obtained from the momentum equations solved. With such formulation, it is neglected transient periods of air velocity reorganization from the stationary field without rotation (static HPC) to the field with pronounced rotation effects when HPC starts to operate and back when HPC stops. However, as the HPC angular speed is 30 rpm these transient periods do not exceed several seconds.

The scenario of the CO_2 transport problem computations is as follows. First, the sample of 15 min is computed using the "frozen" velocity field taking into account the HPC rotation. This basic "frozen" velocity field for this sample was an instantaneous velocity field extracted from the data computed for Case 2. This instantaneous field is

extracted from the period of the statistically-developed flow. The cabin initial $ppCO_2$ value of 3.0 mmHg and temperature value of 72°F were set.

Starting from the end of the first sample, the second sample of 15 min was computed using the "frozen" velocity field computed for Case 1 without rotation. The final CO_2 field obtained for the first sample was used as the initial field for the second one.

Presence of two crewmembers placed in PMM was modeled directly by two point CO_2 sources. The CO_2 generation rate assumed for the assisting crew metabolic respiration was set to 2.2 lbm/day. The CO_2 generation rate assumed for the exercising crew metabolic respiration during 15 minutes of HPC operation was two times higher than in case of normal activity, 4.4 lbm/day. During the next 15 minutes of rest this crewmember also generates 2.2 lbm/day of CO_2.

The operation of CO_2 removal systems and the CO_2 generation by another crew outside PMM were neglected. So it was assumed that "clean" air with ppCO2 of 3.0 mmHg supplying through IMV ducting (130 cfm) is mixed with 115 cfm of air from return grilles and the mixture is provided to the cabin through the diffusers. The mixing procedure has been modeled by means of a specialized ANSYS FLUENT User Defined Function (UDF)[6] that defines the inlet $ppCO_2$ boundary conditions on the diffuser surfaces using $ppCO_2$ values averaged over the correspondent outlet sections.

C. Computational Aspects and Turbulence Modeling

The computational grid generated for the PFE discharge CFD modeling is fully unstructured with tetrahedral mesh elements. The tetrahedral grids were created using the GAMBIT 2.4.6 generator.[8] The grids are clustered to the solid walls and to the diffusers. As well, clustering was performed for the region near the ammonia exhaust surface in the U.S. Laboratory.

The FLUENT solver, being face-based, supports polyhedral cells.[5] The advantages that polyhedral meshes have shown over some of the tetrahedral or hybrid meshes is the lower overall cell count, almost 3-5 times lower for unstructured meshes than the original cell count, keeping the same spatial accuracy.

Conversion of the initial tetrahedral grid to polyhedral one was performed in FLUENT, see Ref. 6 for details. The clustering of the grids to the walls and to the diffusers was kept during the conversion procedure. The final polyhedral grid consisted of about 3,900 thousand cells (that corresponds to more than 22 million nodes).

The Unsteady Reynolds-Averaged Navier-Stokes (URANS) approach was employed. The RANS-based modeling approach greatly reduces the required computational effort and resources, and is widely adopted for practical engineering applications. For the ISS ventilation case, a comparison of the Columbus experimental data with the results of 3D steady-state RANS computations as well as with the accurate Large Eddy Simulation computations prove that RANS modeling is quite accurate regarding to air ventilation velocity field.[9]

The realizable k-ε model[10], with the standard wall functions[11], was used for computations. The wall distance of a cell centre adjacent to a solid wall measured in wall units, y_p^+, ranged from 10 to 50 over the majority of the solid walls. The inlet turbulence intensity was taken as 10% for all the diffusers while the inlet ratio of the turbulent to molecular viscosity, ν_{tur}/ν, was varied from diffuser to diffuser to ensure that the inlet-jet effective Reynolds numbers, $Re_{eff} = V_{in}L_s/(\nu+\nu_{tur})$, are within the range from 200 to 300. Here V_{in} is the inlet velocity value, and L_s is the inlet length scale (the diffuser width).

The governing equations for conservation of mass, momentum, CO_2 transport, and turbulence characteristics were solved using the unsteady segregated pressure-based solver.[6] The SIMPLEC pressure-velocity coupling scheme was used. The second-order upwind spatial discretization scheme was used, for the momentum and the k-ε model governing equations. The second-order pressure interpolation scheme was employed. The under-relaxation factors of 0.8 were set for the pressure and turbulence characteristics, while for the momentum the under-relaxation factor was 0.9.

The second order implicit transient formulation was used. For the unsteady simulation of airflow (Case 2) the time step of 0.0333 seconds was used that corresponds to 60 steps for each revolution. The sample of three minutes was computed for Case 2. For the unsteady simulation of the CO_2 transport in the "frozen" velocity field the time step of one second was used. It allowed to compute the total sample of 30 minutes.

For numerical simulation acceleration, parallel computations were performed using eight processes of a LINUX-based cluster.

III. Results and discussion

To present air velocity and carbon dioxide concentration fields, four plane slices were extracted from the computational domain. The plane slices are shown in Fig. 1d (X-direction indicates the aft-forward direction, Y-

direction indicates the port-starboard direction, and Z-direction indicates the zenith-nadir direction; the centre of the ISS coordinate system used is in the centre of Node 1 radial bay). Two cross sections, S1 and S2, are the diagonals of the module. Another two cross-sections, S3 and S4, are the X and Y mid-sections of the module.

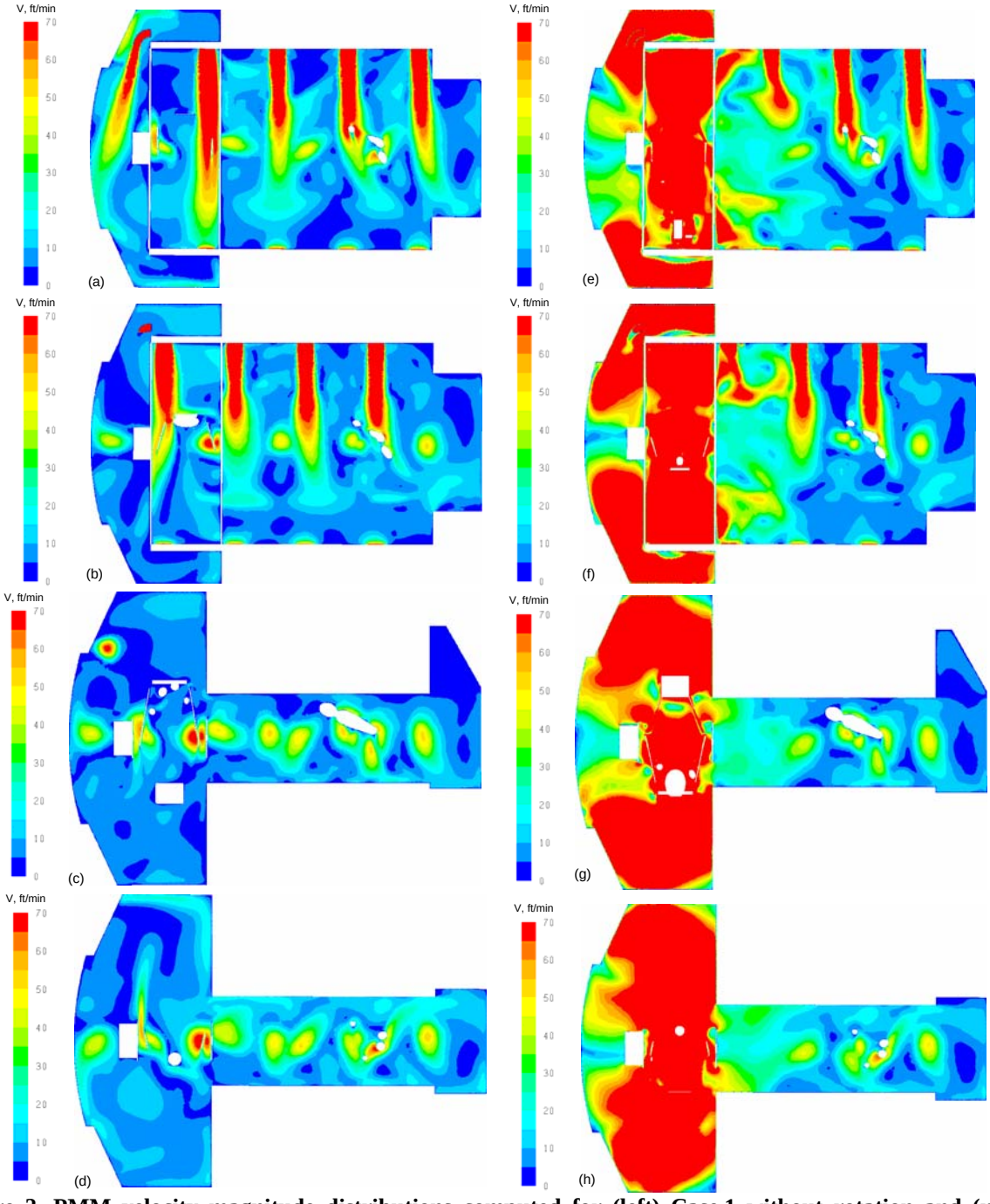

Figure 2. PMM velocity magnitude distributions computed for (left) Case 1 without rotation and (right) Case 2 with rotating HPC and ECLOID in Bay 4: (a,e) diagonal slice S1; (b,f) diagonal slice S2; (c,g) slice x =0; (d,h) slice y = 0.

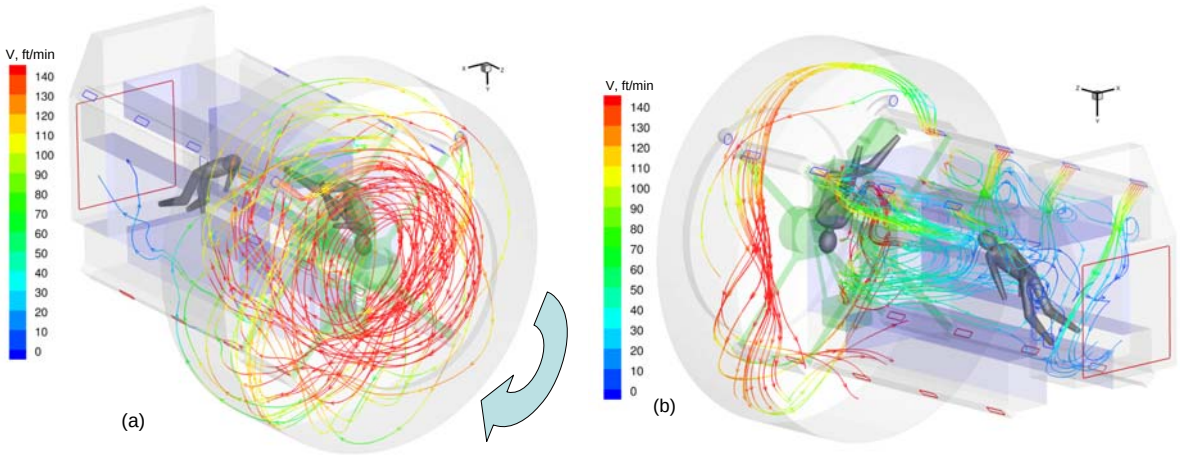

Figure 3. Pathlines colored with velocity magnitude for an instant when the crew is exercising, Case 2: (a) issued from the PMM endcone diffusers; (b) issued from the PMM main air supply diffusers.

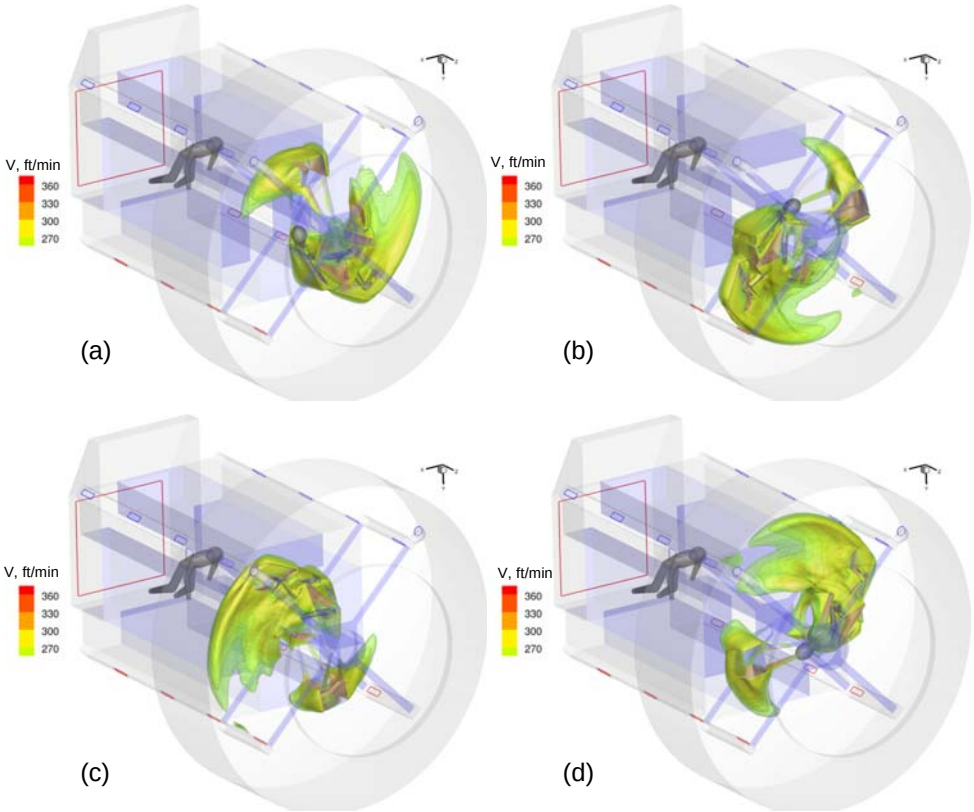

Figure 4. Instantaneous isosurfaces of air velocities computed for Case 2 presented for the instants of (a) T_0, (b) T_0 + 0.5 s, (c) T_0 + 1 s, (d) T_0 + 1.5 s.

Fig. 2 shows velocity magnitude scalar plots at the plane sections considered. It is visible that if HPC is operating (Case 2) air velocities in Bay 4 are very high. Intensive air flow in this region is produced by the rotating equipment and human body. It is in accordance with the estimation of linear velocities of the rotating equipment at the periphery of Bay 4 for the adopted angular velocity of 30 rpm: the level of linear velocities is about 600 ft/min at radius of 1 m.

Fig. 3 and 4 also illustrate velocity field for Case 2 when HPC is operating (note that the air velocity field illustrated in Fig. 3 was used for the CO_2 transport computations during the period of HPC operation). Pathlines issued from the endcone diffusers demonstrate that the flow in Bay 4 is fully-dominated by the rotation (see Fig. 3a).

Air from the main air supply diffuser located in Bay 4 is also involved into the rotating core, see Fig. 3b. Moreover, HPC rotation forms a global flow structure in the PMM cabin: air from the main air supply diffusers in Bays 2 and 3 turns towards endcone direction due to suction effect of the near-HPC rotating flow, see pathlines in Fig. 3b.

Fig. 4 shows isosurfaces of high air velocities exceeding 270 ft/min for one full revolution of the HPC (time interval between successive plots is 0.5 s that corresponds to a 90-degree turn of the crew-bike system). Isosurfaces of high velocities visible in the plots correspond to the trace behind the human body and the massive parts of the HPC equipment. Interestingly the isosurface does not change its shape and volume much from one position to another. The trace behind the human body is almost the same for each position.

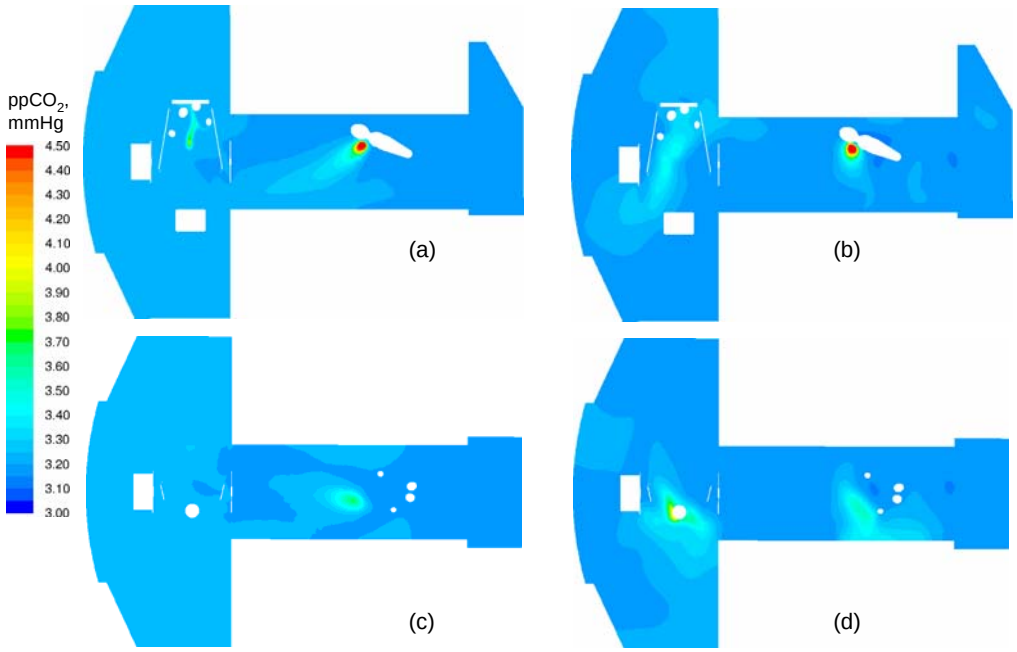

Figure 5. Carbon dioxide content at two time instants: (left) t = 15 min, the end of HPC operation period; (right) t = 30 min, the end of crew rest period (without HPC rotation). (a,b) slice x = 0, (c,d) slice y = 0.

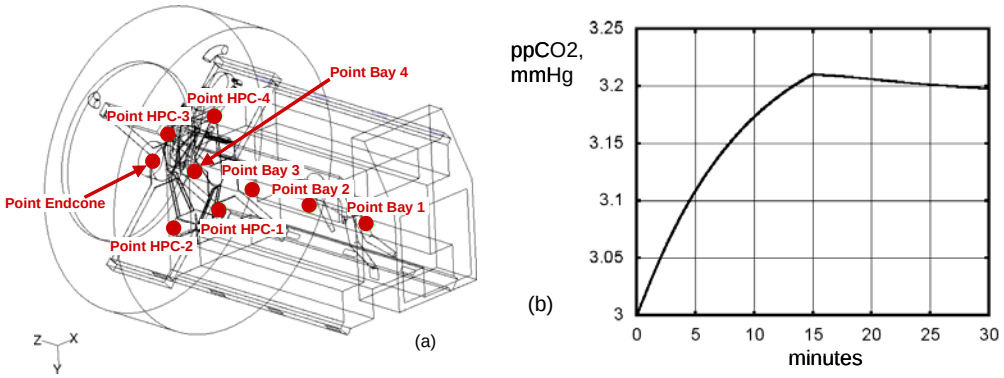

Figure 6. (a) Monitoring points positions. (b) Volume-averaged carbon dioxide concentration evolution.

Instantaneous distributions of $ppCO_2$ are given in Fig. 5 for two instants: the first one corresponds to the period of HPC operation when the rotation effects are significant, and the second one corresponds to the end of the crew rest period with immovable HPC equipment. It is visible that though the CO_2 generation rate for the exercising crew is two times higher than in case of normal activity, additional mixing due to rotation weakens formation of a high-CO_2 plume in the vicinity of the astronaut face (Fig. 5a,c). The shape of the plume near the assisting crewmember confirms the conclusion that when HPC is operating the flow direction in the centre of the cabin aisle way is directed towards the endcone (Fig. 5a). Quantitative analysis of the $ppCO_2$ field allowed to conclude that the plume with $ppCO_2 > 7$mmHg is very small for both the crewmembers. This plume is almost completely removed near the exercising astronaut during the HPC operating period.

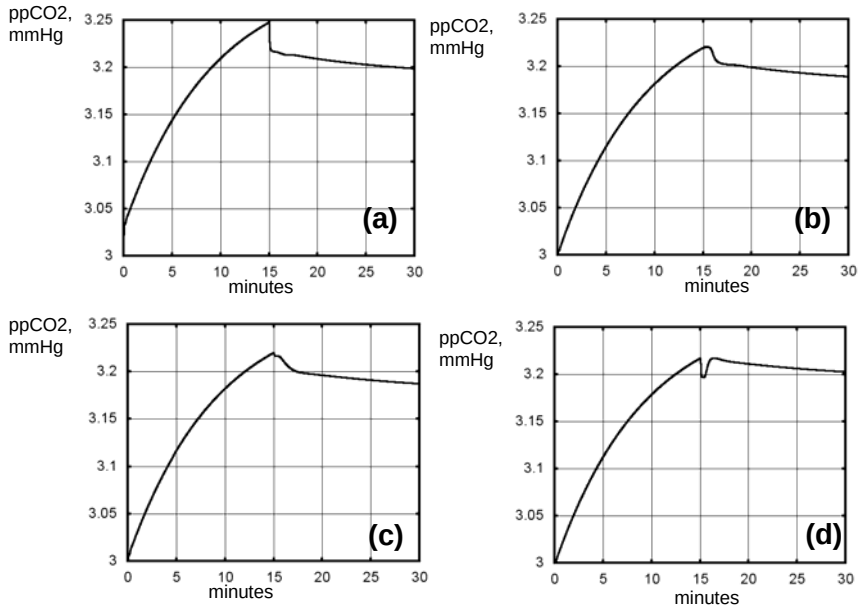

Figure 7. Carbon dioxide concentration evolution at four monitoring points located in Bay 4: (a) point HPC-1; (b) point HPC-2; (c) point HPC-3; (d) point HPC-4.

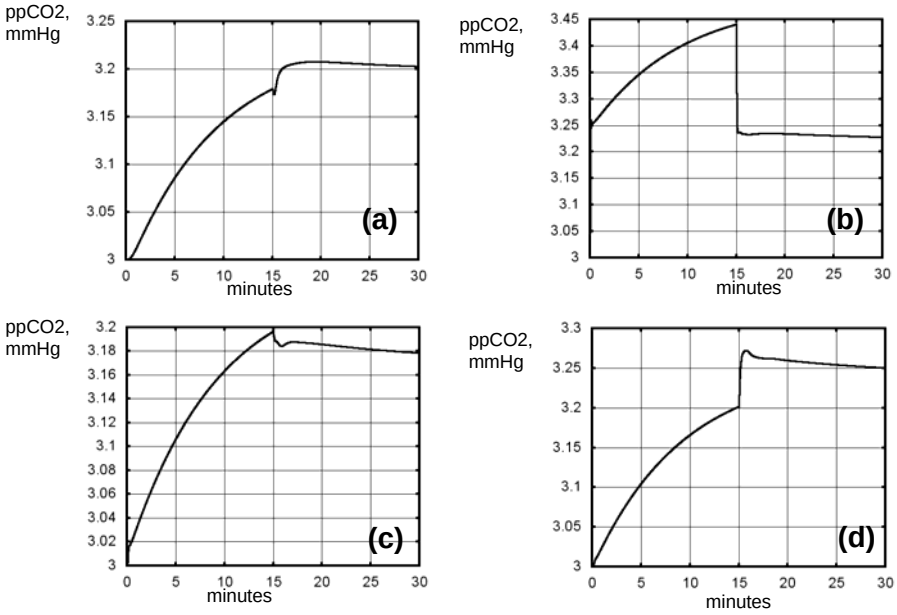

Figure 8. Carbon dioxide concentration evolution at four monitoring points located in the PMM cabin: (a) point Bay 1; (b) point Bay 2; (c) point Bay 3; (d) point Bay 4.

The volume-averaged $ppCO_2$ evolution plot is given in Fig. 6b. It is visible that the peak value of the CO_2 content is at the end of the HPC operation period ($ppCO_2$ of about 3.2 mmHg). The local effects of the carbon dioxide transport are illustrated additionally in Fig. 7 and 8. The carbon dioxide evolution plots at the monitoring points near HPC (in the rotating core) are presented in Fig. 7, while Fig. 8 gives the plots for the monitoring points that are located in the PMM cabin regions without strong rotation effect (far from HPC). The monitoring point position is shown in Fig. 6a. It is visible that the highest $ppCO_2$ level during the exercise period is not in Bay 4, it is reached in Bay 2 where the assisting crewmember is placed. The reason is in the flow field from the main supply diffusers illustrated in the pathline plots (see Fig. 3b). The global ventilation structure formed in the PMM cabin when the HPC is rotating worsens ventilation in Bay 2 that leads to local increase of the CO_2 content. After the

rotation is stopped, better ventilation in Bay 2 is provided that immediately leads to reduction of the CO_2 concentration (see Fig. 8b). On the contrary, as it is visible in Fig. 8a,d, the CO_2 content in Bay 1 and in the center of Bay 4 increases after the HPC rotation stops, but not too much. In general it could be concluded that there is no concern on high-CO_2 bubble formation in the vicinity of the exercising crew, but carbon dioxide content near the assisting crew could be a concern.

IV. Conclusion

ISS ventilation characteristics for PMM with the Human Powered Centrifuge operation were numerically predicted using the CFD software FLUENT 12.1. The air flow pattern and CO_2 content in the PMM cabin aisle way were modeled to provide a detailed analysis of CO_2 transport during a half-an-hour period: 15 min of crew exercising with the following 15 min of crew rest.

The computational data obtained allowed concluding that there is no considerable risk of stagnant zones formation within PMM cabin. On the contrary, due to rapid rotation of the exercising crew body and the massive parts of the HPC equipment PMM cabin air velocities are very high. During crew exercising period velocity level in some regions of PMM Bay 4 is higher than of 300 ft/min. HPC operation influence the flow structure in Bays 2 and 3 as well: airflow from the main supply diffusers turns towards endcone direction due to suction effect of rotating flow in Bay 4.

Carbon dioxide partial pressure gradients are relatively high as the exercising and the assisting crewmembers are present in the specific positions for a long time. Intensive air mixing due to rotation eliminates the risk of high-CO_2 bubble formation in the vicinity of the exercising crew. The only concern is the carbon dioxide content near the assisting crew during the HPC operating period. However, detailed analysis of the carbon dioxide concentration fields allowed to conclude that the plume with $ppCO_2 > 7$mmHg is very small for both the crewmembers.

References

[1]Clement, G., *Fundamentals of Space Medicine*, Springer, New York, 2011. 381 p.

[2]Clement, G., and Bukley, A. (eds), *Artificial gravity*, Springer, New York, 2007. Chap. 3.

[3]Yang, Y., Kaplan, A., Pierre, M., et al., "Space Cycle: A Human-Powered Centrifuge that can be used for hypergravity resistance training," *Aviation, Space, and Environmental Medicine*, Vol. 78, No 1, 2007, pp. 2-9.

[4]Caiozzo, V.J., Rose-Gottron, C., Baldwin, K., et al., "Hemodynamic and metabolic responses to hypergravity on a human-powered centrifuge," *Aviation, Space, and Environmental Medicine*, Vol. 75, No 2, 2004, pp. 101-108.

[5]European Space Agency (2010). "Permanent Multipurpose Module" http://www.thalesaleniaspace-issmodules.com/pmm. [cited 21 March 2012]

[6]ANSYS FLUENT 12.0 Theory Guide. Release 12.0. ANSYS, Inc. January 2009.

[7]GAMBIT 2.4 Modeling Guide, Fluent Inc., 2007.

[8]Smirnov, E.M., Ivanov, N.G., Telnov, D.S., and Son, C.H., "CFD modeling of cabin air ventilation in the International Space Station: a comparison of RANS and LES data with test measurements for the Columbus Module," *Int. J. of Ventilation*, Vol. 5, No 2, 2006, pp. 219-228.

[9]Shih, T.-H., Liou, W.W., Shabbir, A., Yang, Z., and Zhu, J. "A New k-ε Eddy-Viscosity Model for High Reynolds Number Turbulent Flows - Model Development and Validation," *Computers Fluids*, Vol. 24, No 3, 1995, pp. 227-238.

[10]Launder, B.E., and Spalding D.B., "The numerical computation of turbulent flows," *Computer Methods in Applied Mechanics and Engineering*, Vol. 3, 1974, pp. 269-289.